

# On the Geomagnetic storm on February 11, 1958

By

M. NAGAI

## Abstract

The great geomagnetic storm which occurred at 01 h 25 m UT Feb. 11, 1958, was analysed using the data of 28 station's hourly values during 3 days from  $-24$  hr to  $+48$  hr of the SC. And the equivalent current vectors of the DS field were compared with the world-wide patterns of the blackouts. From this study three remarkable characteristics deduced as follows.

- (1). The most active DS field happened suddenly one hour after the SC ( $+1$  hr) almost all over the auroral zone and the polar cap. This is an exceptional characteristic compared with the other IGY storms with sudden commencements, of which DS fields grew generally with the development of the Dst field.
- (2). Polar cap blackouts began to occur 13 hours before the SC ( $-13$  hr). The horizontal component of the geomagnetic field, which had been almost calm until this time, began to decrease simultaneously. The pre-sc disturbance reached the maximum stage 6 hours before the SC ( $-6$  hr). At that time, observed H decreases reached 500 gammas approximately, at the auroral zone stations, College, Tiksy and Dixon.

The rotational trends of the distribution of the equivalent current vectors of the pre-sc disturbance at  $-11$  hr and  $-1$  hr were clockwise on the morning side and counterclockwise on the evening side. Then it was concluded that the current systems of the initial phase were equivalent to the intensified pre-sc current systems.

- (3). The southward shift of the auroral zone was observed clearly associated with the development of Dst. In the developing stage of the Dst until the maximum at  $+9$  hr, the southward shift of the auroral zone was observed in the European zone on the morning side, while in the recovering stage of the Dst since  $+9$  hr the shift was observed in the zone from Alaska to Kamchatka with a distribution of spiral pattern. And the red homogeneous arc of aurora was observed at Memambetsu ( $\phi_m=34.1$ ) in Japan during the period from 19 h to 22 h LT.

## § 1. Introduction

The geomagnetic storm on February 11, 1958 was the greatest among the storms which occurred during the IGY. Its maximum range of H amounted to  $617\gamma$

at Kakioka. Before the occurrence of the storm, a solar flare of importance 2 (S 13° W 14°) occurred at 21h 08m UT, February 9, accompanying an outburst of Type IV.

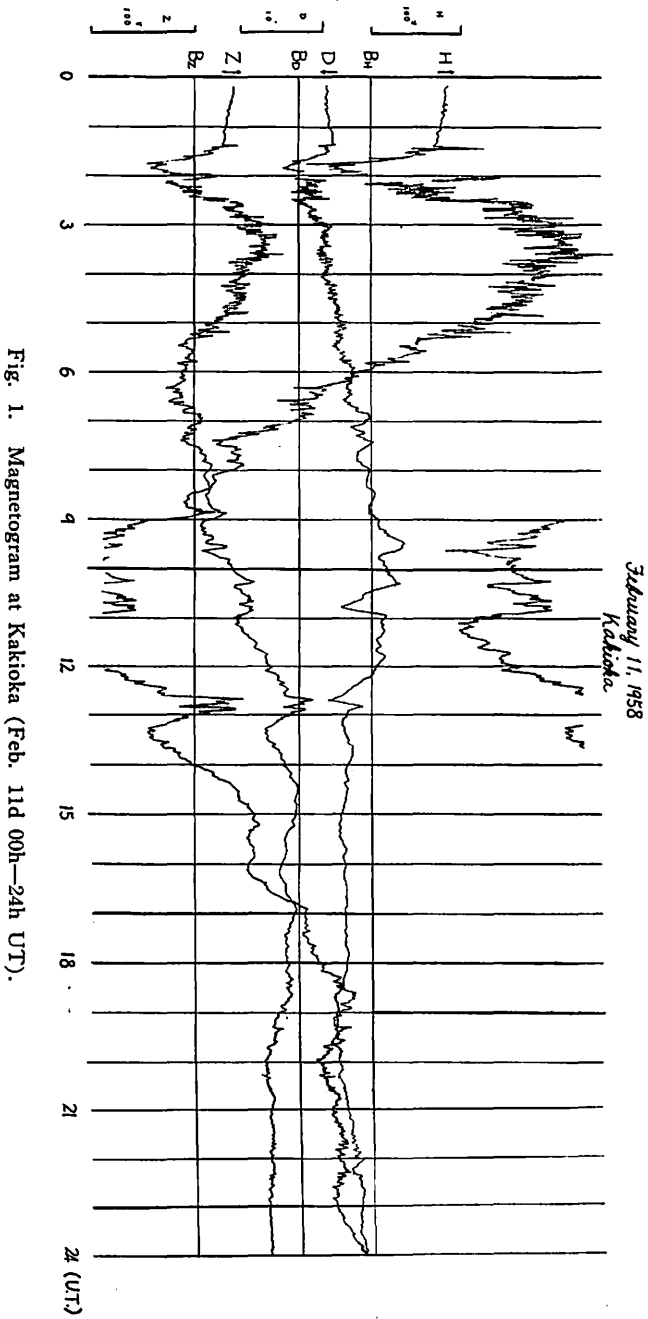


Fig. 1. Magnetogram at Kakioka (Feb. 11d 00h—24h UT).

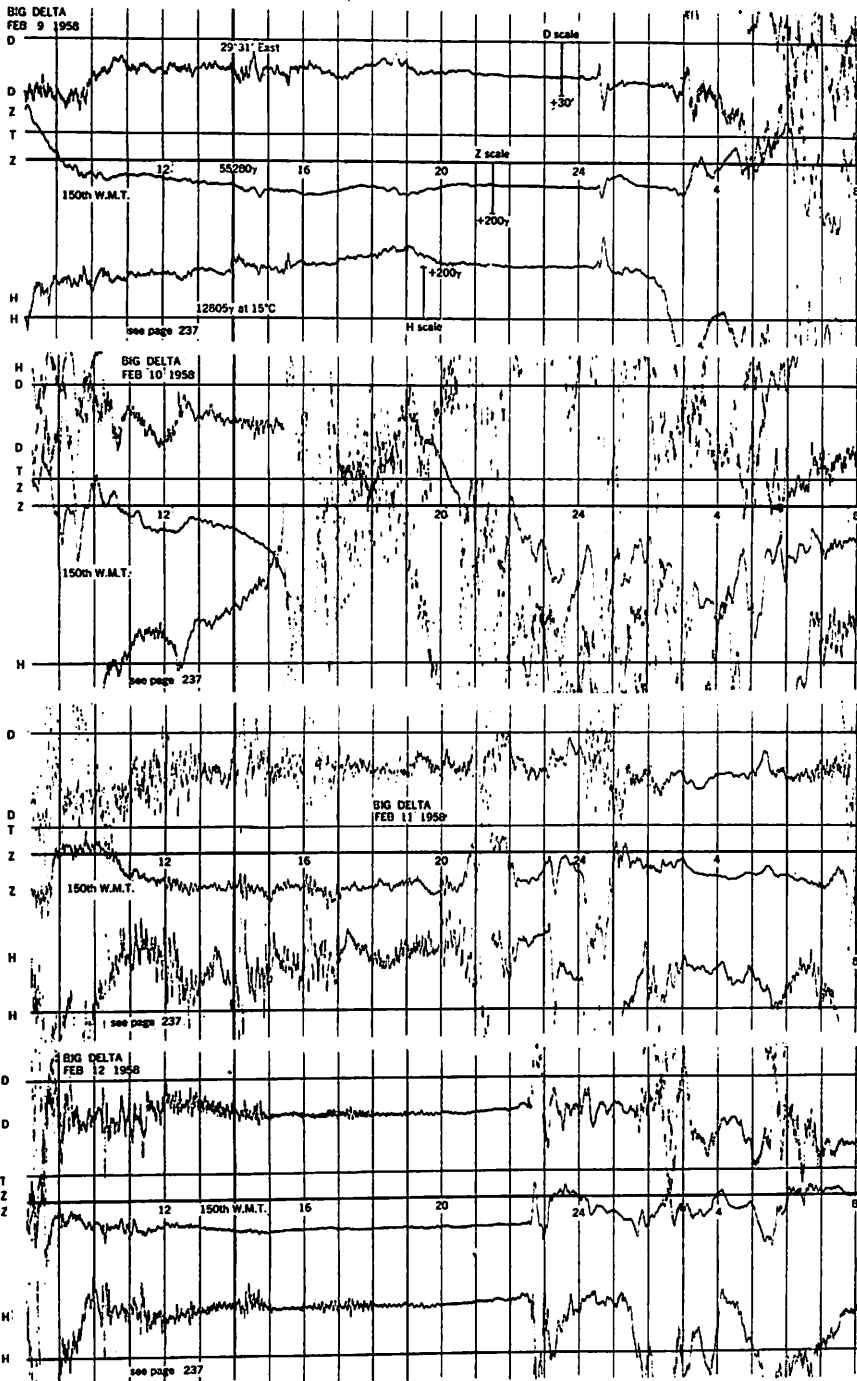


Fig. 2. Magnetogram at Big Delta (Feb. 9<sup>00</sup>8<sup>h</sup>—13<sup>00</sup>8<sup>h</sup>, 150 th W. M. T. )

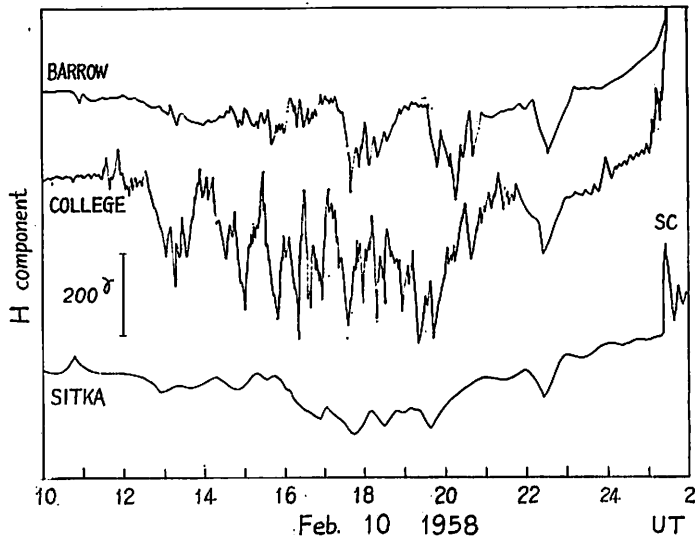


Fig. 3. Variations of the horizontal component in the pre-sc stage at three stations, Barrow, College and Sitka.

The time interval  $\Delta T$  between the flare and the SC of the storm was about 28 hours ( $1.5 \times 10^8$  km/s).

Polar cap blackouts occurred 13 hours before the SC and continued by about 34 hours until to the last phase of geomagnetic storm.

## § 2. Characteristics of this storm deduced from the inspection of the magnetograms

Fig. 1 shows the magnetogram of the storm at Kakioka. The sudden commencement ( $\Delta H$ ,  $+62 \gamma$ ) of this storm occurred at 01 h 25 m UT, February 11, 1958 and soon later there was a decrease of  $130 \gamma$  in H component. The second sharp increase ( $\Delta H$ , about  $+150 \gamma$ ) took place at 01 h 59 m, and the initial phase continued about 3 hours. During the initial phase, rapid oscillations with periods of 3~5 minutes were observed. This activity suggests more intense DS fields than the normal storms during the IGY.

Fig. 2 shows the magnetogram at Big Delta (Feb. 9 d 08 h~13 d 08 h, 150 th W.M.T.). A sudden impulse like sudden commencements in the low latitudes was observed at 10d 00h 35m, 150th W.M.T., that is 15 hours before the SC, 10d 15h 25m, 150 th W.M.T. And the horizontal component decreased at about 02h, one and half hours later. This decrease coincides with the time of the beginning of polar cap blackouts in the day time.

Station	Geomagnetic Latitude $\phi_m$	Maximum Range $\Delta H\gamma$	Maximum Time (storm time)
Barrow	68.6	-200	- 5 hr
College	64.5	-500	- 7 hr
Sitka	60.0	-200	- 8 hr

Fig. 3 shows the variations of the horizontal component in the pre-sc stage. The maximum ranges of the pre-sc disturbance at three stations are as follows.

At Barrow and College, rapid irregular variations superposed on the pre-sc disturbances were observed, but at Sitka those rapid variations were rather small. This shows that the active zone of the pre-sc disturbance is restricted in a very sharp narrow zone of auroral latitudes.

### § 3. Analysis of hourly values

Fig. 4 shows the Dst obtained from mean values of the 6 stations at the average geomagnetic latitude  $\phi_m=32.5^\circ$ . The stations are Kakioka, Honolulu, Tucson, San Fernando and Tibilis. In the pre-sc stage, the Dst decrease of about 60 gammas can be seen. Fig. 4 shows also the horizontal intensity  $\sqrt{\Delta X_m^2 + \Delta Y_m^2}$ , the geomagnetic north component  $\Delta X_m$ , and the horizontal disturbance vectors at Thule ( $\phi_m=88.0$ ). These figures clearly show the occurrence of the very active DS soon after SC.

Fig. 5 shows the variations of  $\Delta X_m$  at College and Sitka.  $\Delta X_m$  at College in the pre-sc disturbance is greater than that at Sitka. However,  $\Delta X_m$  at the Dst maximum stage is smaller at College than Sitka.

Fig. 6 shows the variations of  $\Delta X_m$  at Dixon, Tiksy and Lerwick. The pre-sc disturbances at Dixon and Tiksy are distinct. But it is not so clear at Lerwick, though the DS in the initial phase is active there.

Fig. 7 shows the variations of  $\Delta X_m$  at Tromsø, Dombas, Lovö, and Rude Skov. Pre-sc disturbances at Lovö and Rude Skov are smaller than Dst's. At Rude Skov active DS in the initial phase are not seen. Because of the southward shift of the auroral zone current jet, Tromsø's  $\Delta X_m$  becomes smaller at the time of Dst maximum.

The maximum ranges of  $\Delta X_m$  in the pre-sc stage, the initial phase and the Dst maximum stage are given in the following table for the several stations concerned.

Fig. 8 shows the southward shift of the auroral zone current jet assuming a line

Station	Geomagnetic Latitude $\phi_m$	Pre-sc stage	Initial phase	Dst Maximum stage
College	64.5	-500 $\gamma$	+600 $\gamma$	-1000 $\gamma$
Sitka	60.0	-200	+650	-1300
Dixon	63.0	-450	+400	-550
Tiksi	60.5	-500	+250	-350
Lerwick	62.5	+100	-800	-650
Troms $\phi$	67.1	-150	-1400	-200
Dombås	62.3	-100	-650	-600
Lov $\delta$	58.1	-50	-700	-450
Rude Skov	55.8	-50	-50	-400

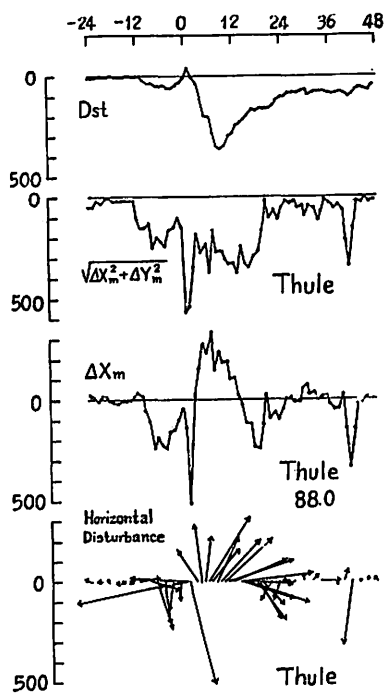


Fig. 4. The Dst ( $\Delta X_m$ ) curve for the storm of February 11, 1958. And the curves of the horizontal intensity the geomagnetic north component  $\Delta X_m$  and the horizontal disturbance vectors at Thule ( $\phi_m=88.0$ ).

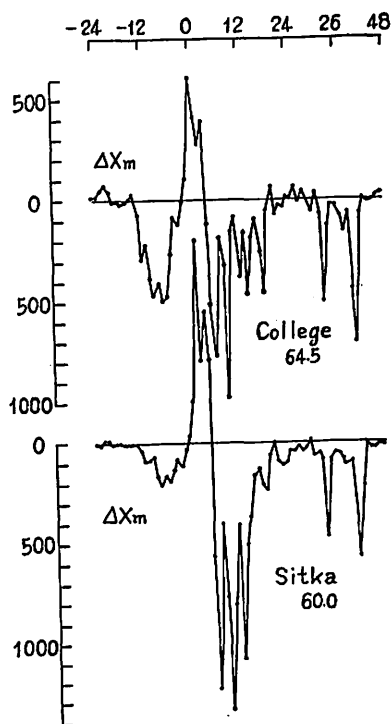


Fig. 5. The curves of  $\Delta X_m$  at College and Sitka.

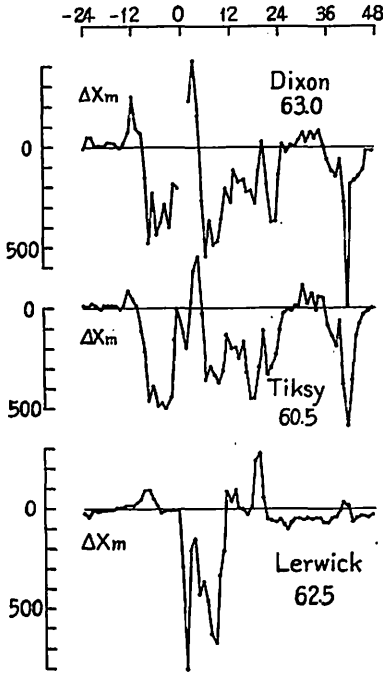


Fig. 6. The curves of  $\Delta X_m$  at Dixon, Tiksy and Lerwick.

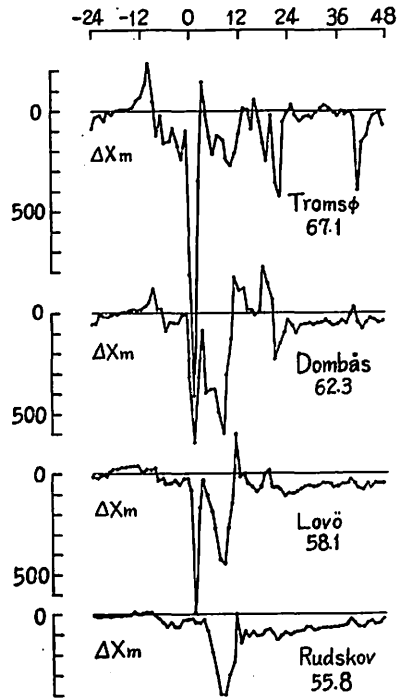


Fig. 7. The curves of  $\Delta X_m$  at Tromsø, Dombås, Lovö and Rude Skov.

$\Delta X_m \cdot \Delta Z$

$\Lambda$	$\phi$		0	1	2	3	4	5	6	7	8	9	10	11	12	13	14	15	16	17	18	19	20	21	22	23
255.4	645	College	X	O	X	X	O	X	⊙	⊙	O	X	?	O	?	O	O	?	O	X	O	X	X	X	X	X
258.1	609	Anchorage	X	X	X	X	X	X	X	X	X	X	O	O	O	O	O	O	O	X	X	X	X	X	X	X
275.4	600	Sitka	X	X	X	X	O	X	X	?	O	X	O	O	O	X	O	X	O	?	X	X	X	X	X	X
191.4	605	Tiksy	X	X	X	X	O	?	X	X	O	O	X	X	?	X	?	O	O	O	O	X	O	O	O	O
161.5	630	Dixon	-	-	X	X	O	X	X	X	X	X	X	X	O	O	O	O	O	O	O	X	O	O	O	O
116.7	67.1	Tromsø	O	O	X	X	X	O	X	X	X	O	O	O	O	O	O	O	O	X	X	X	X	X	X	X
100.0	623	Dombås	X	X	X	X	O	O	O	O	X	O	X	X	X	X	X	X	X	X	X	X	X	X	X	X
105.8	58.1	Lovö	X	X	X	X	X	O	O	O	X	X	X	X	X	X	X	X	X	X	X	X	X	X	X	X
98.9	55.8	Rudskov	X	X	X	X	X	X	X	⊙	O	X	X	X	X	X	X	X	X	X	X	X	X	X	X	X
88.6	625	Lerwick	X	X	X	X	O	O	O	O	X	X	/	X	X	X	X	X	X	X	X	X	X	X	X	X
82.9	585	Eschscholtz	X	X	X	X	X	X	X	X	O	?	X	X	X	X	X	X	X	X	X	X	X	X	X	X
79.0	546	Hartland	X	X	X	X	X	X	X	X	X	X	?	X	X	X	X	X	X	X	X	X	X	X	X	X

Fig. 8. The southward shift of the auroral zone current jet when a line current is assumed

- :  $\Delta X_m \cdot \Delta Z < 0$       The current jet is in the south of the station.
- × :  $\Delta X_m \cdot \Delta Z > 0$       The current jet is in the north of the station.
- ⊙ :  $\Delta X_m \cdot \Delta Z = 0$       The current jet is just over the station.

current. In the figure the mark  $\circ$  shows the case of  $\Delta X_m \cdot \Delta Z < 0$ , that the auroral zone current jet is in the south of the station. The mark X shows the case of  $\Delta X_m \cdot \Delta Z > 0$ , that the auroral zone current jet is in the north of the station, and the mark  $\odot$  shows  $\Delta X_m \cdot \Delta Z = 0$  that the current jet is just over the station.

In the developing stage of Dst before the maximum at +9<sup>hr</sup>, the auroral zone current jet extended to the south of Rude Skov in the European zone of the geomagnetic longitude about 100°. And it extended clearly to the south of Sitka in the recovering stage after +10<sup>hr</sup>. This southward shift of the auroral zone current jet well coincided with that of the impact zone of the auroral zone blackout.

#### § 4. Characteristics deduced from the current vector

In this section, the patterns of development of the blackout and the current vector are shown for each stage.

In order to draw the current vectors, hourly values of 28 geomagnetic stations in the northern hemisphere are used. The names, the abbreviations, the locations, and other elements of these observatories are given in Table 1.

The world-wide patterns of polar blackouts have already been obtained by the analysis of  $f_{min}$  data of 49 ionospheric sounding stations. (1) The locations of these

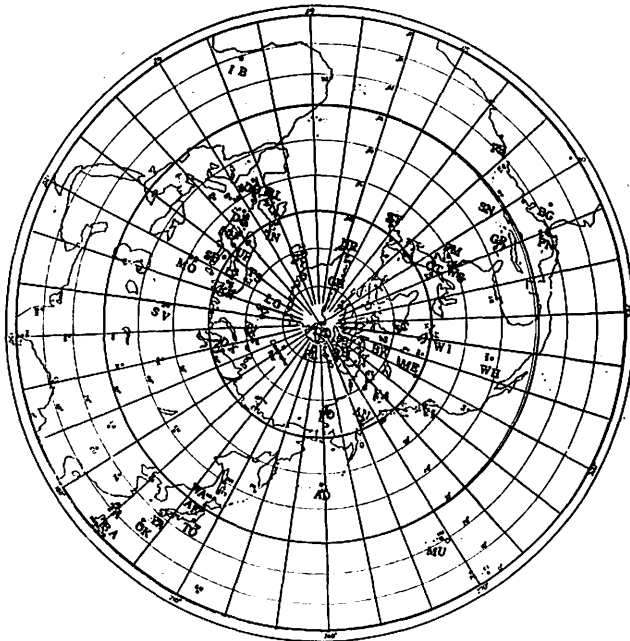


Fig. 9. Distribution of ionospheric sounding stations.

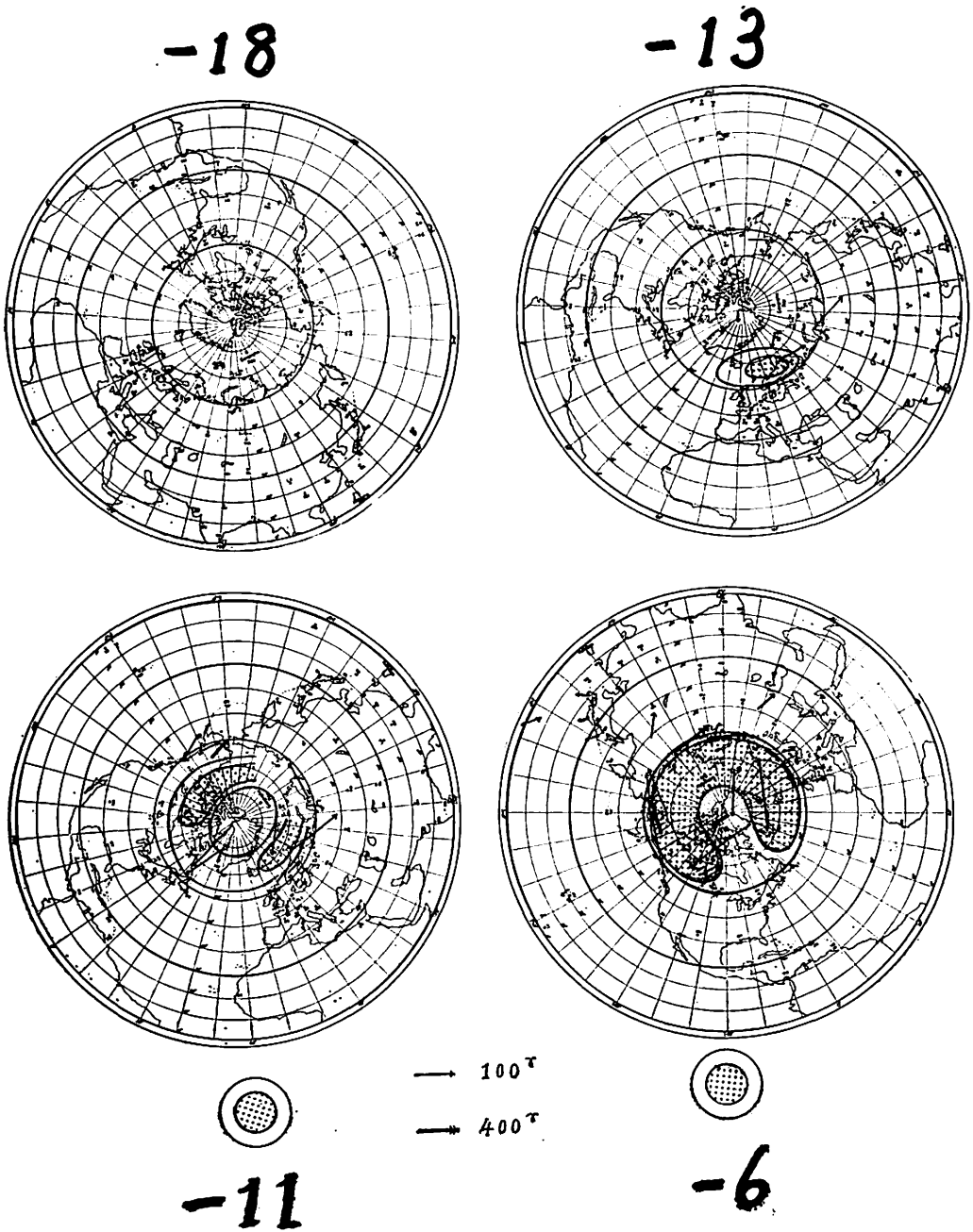


Fig. 10. The patterns of the development of the blackout and the current vector for each stage.

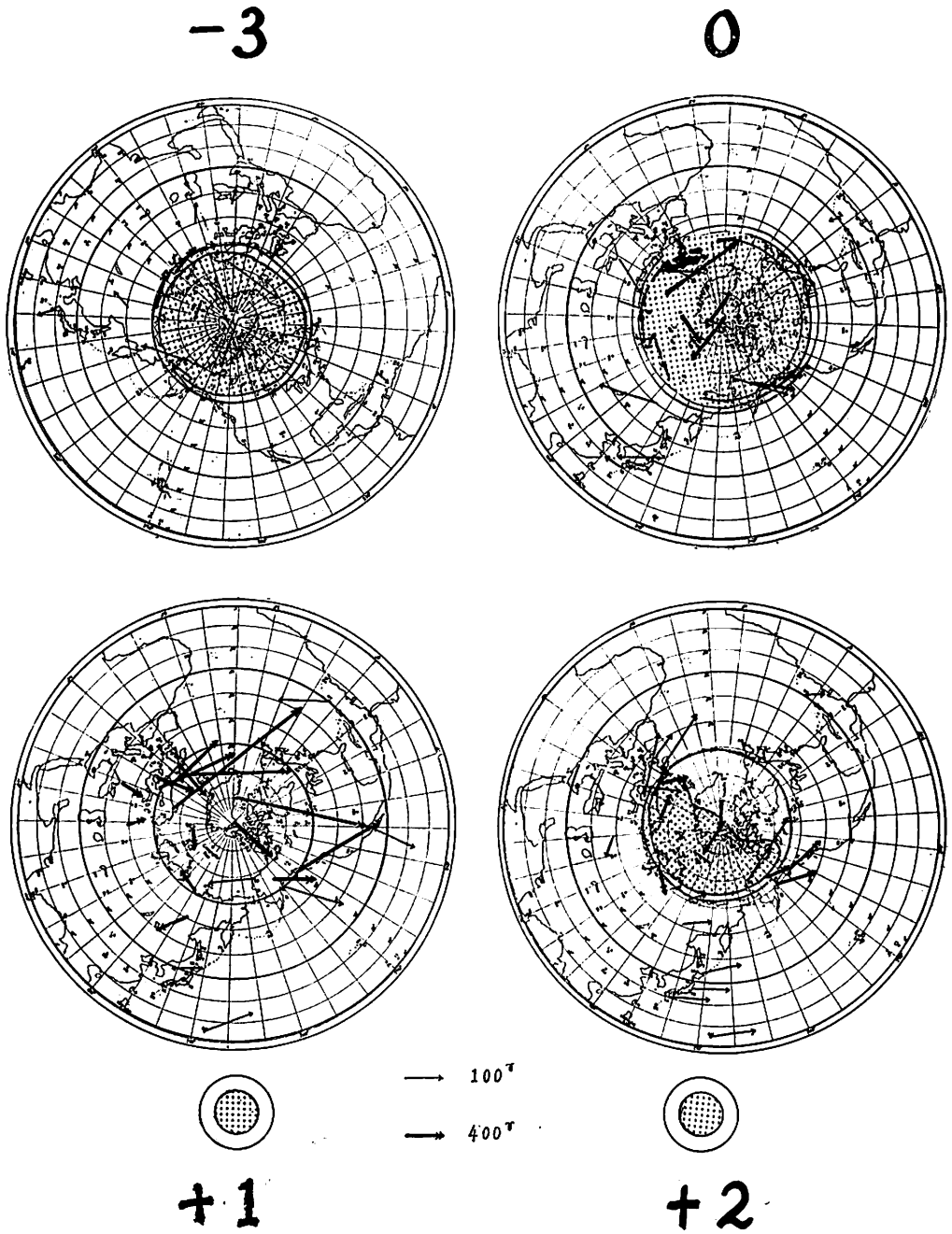


Fig. 11. The patterns of the development of the blackout and the current vector for each stage.

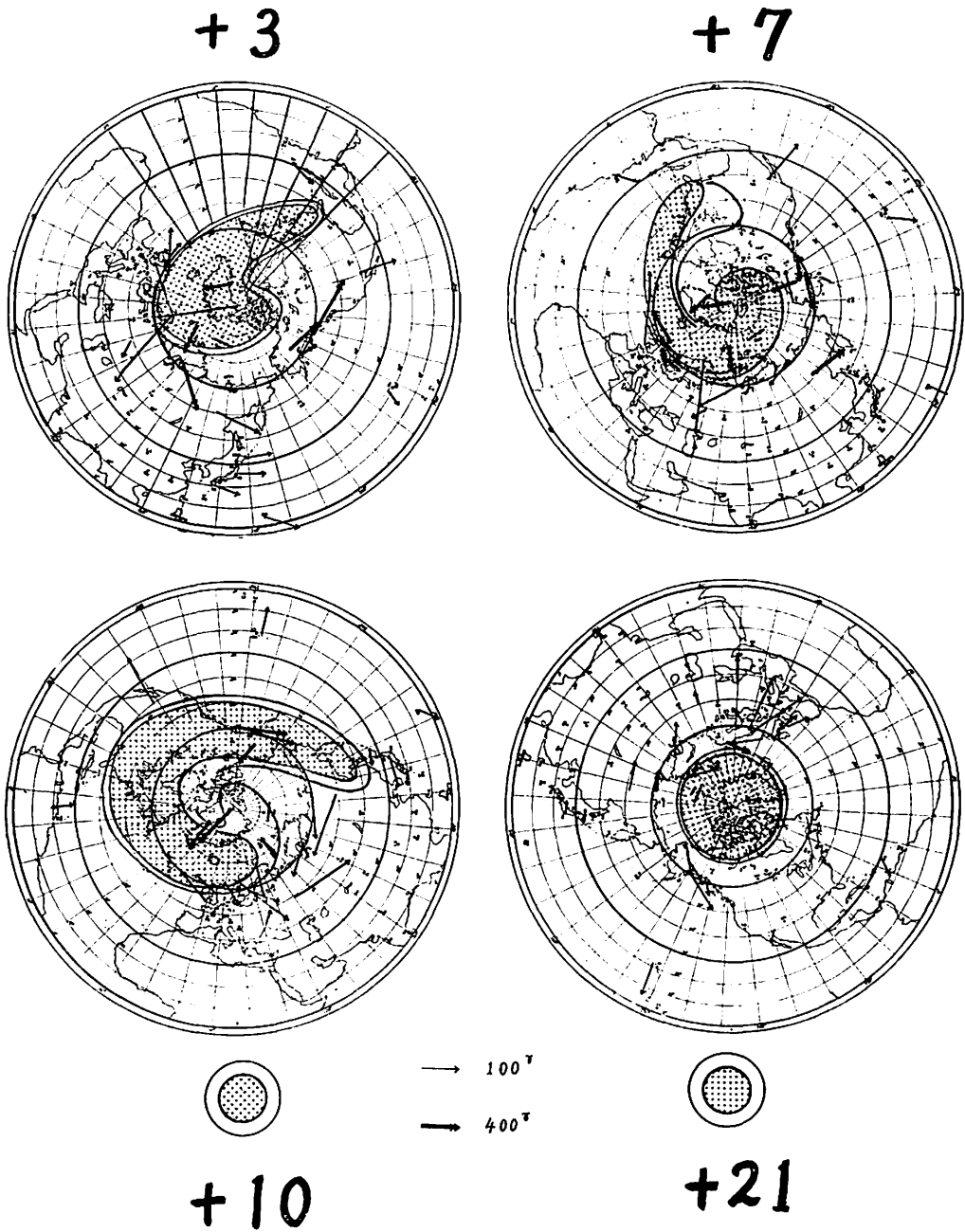


Fig. 12. The patterns of the development of the blackout and the current vector for each stage.

Table 1. List of magnetic observatories

Observatory	abbr.	Geomagnetic		Geographic		$\psi$	D- $\psi$
		Lat. $\phi$	Long. $\Lambda$	Lat. $\phi$	Long. $\lambda$		
Thule	Th	88.0	0.0	77.5	291.0	0.0	-79.7
Godhavn	Go	79.8	32.5	69.2	306.5	-17.5	-34.8
Marchison Bay		75.2	137.2	80.0	18.3		
Point Barrow	PB	68.6	241.0	71.3	203.2	33.0	- 6.5
Tromsø	Tr	67.1	116.7	69.7	18.9	-30.8	29.7
College	Co	64.5	255.4	64.9	212.2	27.0	1.9
Murmansk	Mm	64.1	126.5	69.0	33.0	-26.6	38.0
Dickson	Di	63.0	161.5	73.5	80.4	-12.8	41.8
Lerwick	Le	62.5	88.6	60.1	358.8	-23.6	13.7
Dombås	Do	62.3	100.0	62.1	9.1	-23.6	17.6
Anchorage	An	60.9	258.1	61.2	210.1		
Tiksiy	Ti	60.5	191.4	71.7	128.9	7.2	7.4
Sitka	Si	60.0	275.4	57.1	224.7	21.4	7.8
Eskdalemuir	Es	58.5	82.9	55.2	356.8	-20.4	9.7
Lovø	Lo	58.1	105.8	59.4	17.8	-22.1	22.6
Rude Skov	RS	55.8	98.5	55.8	12.5	-20.6	18.1
Hartland	Ha	54.6	79.0	51.0	355.5	-18.1	9.1
Yakutsk	Ya	51.0	193.8	62.0	129.7	5.8	-13.1
Odessa	Od	43.8	111.1	46.8	30.9	-15.7	17.6
San Fernando	SF	41.0	71.3	36.5	353.8	-13.6	22.6
Tucson	Tu	40.4	312.2	32.3	249.2	10.1	3.2
Tibilisi	Tf	36.7	122.1	42.0	44.7	-13.1	18.3
Memambetsu	Mb	34.1	208.3	43.9	144.2	7.5	-15.7
San Juan	SJ	29.9	3.2	18.4	293.9	- 0.7	- 6.6
Kakioka	Ka	26.0	206.0	36.2	140.2	6.2	-12.6
Honolulu	Ho	21.1	266.5	21.3	201.9	12.3	- 0.7
Kanoya	Ky	20.7	198.1	31.4	150.9	4.2	- 9.2
Guam	Gu	3.9	212.8	13.5	144.8	6.4	- 4.6

Note :  $\phi$  Geomagnetic latitude,

$\Lambda$  Geomagnetic longitude,

$\varphi$  Geographic latitude,

$\lambda$  Geographic longitude,

$\varphi$  The angle formed by the great circle joining the station and the geomagnetic pole with the geographical meridian of the station (east ward positive),

D Declination (for February 1958)

observatories are shown in Fig. 9. The value of  $f_{min}$  increases with the solar corpuscle's bombardment into the lower ionosphere, and sometimes all ionospheric echoes are completely masked. Thus  $f_{min}$  (the deviation of  $f_{min}$  value from the monthly median) is used to analyse the blackouts. The region of the blackout is hatched in the following figures.

Until the time  $-18^{\text{hr}}$ , the geomagnetic condition was quiet.

At  $-13^{\text{hr}}$  a zone of enhanced ionization appeared in the day side of the polar cap.

At  $-11^{\text{hr}}$  the geomagnetic activity increased and the sense of the rotational distribution of the current vector is clockwise on the morning side and counterclockwise on the evening side.

At  $-6^{\text{hr}}$  pre-sc disturbances developed most severely. The intensity of the horizontal vector amounted to 500 gammas at College, Dixon, and Tiksy.

At  $-3^{\text{hr}}$  the polar cap blackout spreaded over the whole polar cap.

At  $0^{\text{hr}}$  the current vector at  $-1^{\text{hr}}$  was intensified, showing clockwise rotation on the morning side and counter clockwise on the evening side.

At  $+1^{\text{hr}}$  DS field was very active and the current vector was so complex and characteristic, as will be seen in the polar current which flows parallel with the meridian of about  $15^{\text{h}} \sim 17^{\text{h}}$  at Thule and Godhavn.

At  $+2^{\text{hr}}$  (initial phase) the direction of the current vector was the same as at  $0^{\text{hr}}$ , that is clockwise on the morning side and counterclockwise on the evening side.

At  $+3^{\text{hr}}$  the transition stage from the initial phase to the main phase began. The polar cap blackout was changing to the auroral zone blackout.

At  $+7^{\text{hr}}$  (main phase) the auroral zone blackout clearly showed a spiral pattern, and current vectors were deformed. The impact zone of auroral zone blackout coincided with the southward shift of the auroral zone current jet obtained from the analysis of  $\Delta X_m \cdot \Delta Z$ .

At  $+10^{\text{hr}}$  (main phase) the spiral pattern of the auroral zone blackout was developed so much and it extended to the near north of Memambetsu ( $\phi_m = 34.1^\circ$ ) in Japan. At this stage, a red homogeneous arc aurora was observed at Memambetsu.

Deformation of the current system was clear.

At +21<sup>hr</sup> (last phase) the current vector showed again clockwise rotation on the morning side and counter clockwise rotation on the evening side.

The polar blackout was existing only in the polar cap.

## § 5. Discussion and conclusion

### 1) On the pre-sc disturbance

The upper limit of the proton energy produced by the solar flare associated with the outburst of Type IV is generally several hundreds MeV, and the flux is the order of  $10^2$  protons/cm<sup>2</sup> · sec. This value is far smaller compared with  $10^{9-12}$  particles/cm<sup>2</sup> · sec (2) of the solar corpuscular stream responsible for geomagnetic storms. Accordingly it has been considered these protons do not produce a world-wide geomagnetic storm, but only impinge into the earth's atmosphere along Störmer orbits.

In this storm, however, the polar cap blackout began at the earlier pre-sc, -13<sup>hr</sup>, and the geomagnetic polar cap disturbance occurred the same time.

The current system at the pre-sc disturbance is essentially the same as the current system of the initial phase. It may be the intensification of the polar cap current system of the  $S_q^p$ -field which was obtained by Nagata and Kokubun (3). It can be concluded that the pre-sc current system is formed in the polar cap region more than several hours before SC in accordance with the polar cap blackout.

### 2) On the DS field

Soon after the SC the very active DS field was observed all over the regions of the auroral zone and the polar cap. Such DS field reached to -1400 gammas at Tromsø ( $\phi_m=67.1$ ) and -700 gammas at Lovö ( $\phi_m=58.1$ ), but at Rude-Skov ( $\phi_m=55.8$ ) it was only -50 gammas. This difference shows the clear boundary between Lovö and Rude Skov. This boundary coincided with that of the impact zone of blackouts.

The polar current of the DS field flows parallel with the meridian of local noon in Chapman's idealized current system, but of about 09h. in Hasegawa's and Vestine's systems, and of about 07.5h in Nagata's and Harang's. (4) However, in this storm, the polar current of the DS field at +1<sup>hr</sup> flows parallel with the meridian of about 15<sup>h</sup>~17<sup>h</sup> at Thule and Godhavn. This is one of the characteristics of this storm which had not been observed in other storms occurred during the IGY. In general DS field develops gradually in accordance with the development of Dst field. (5)

### 3) Southward shift of the auroral zone

It has been known that the auroral zone shifts southwards with the development of Dst field. In this storm, the auroral zone shifted southwards in accordance

with the spiral impact zone of the auroral zone of the auroral zone blackout. The southward shift was observed in the European zone on the morning side at the developing stage of Dst before the maximum at +9<sup>hr</sup>. On the other hand, at recovering stage after +9<sup>hr</sup> the auroral zone blackout shifted southwards to the Alaska~Kamchatka zone, showing the spiral patten. Simultaneously, the red homogeneous arc aurora was observed at Memambetsu ( $\phi_m=34.1$ ) in 19h~22h LT. It must be noted here that the position of the maximum of the current jet extended southwards only to the latitude of about  $\phi_m=60^\circ$ .

#### Acknowledgments

In concluding, the author wishes to express his sincere thanks to Dr. T. Yoshimatsu, Director of the Kakioka Magnetic Observatory and Dr. K. Yanagihara, Chief of the Observation Section of the Observatory for their valuable advices and encouragements and also wishes to thanks Dr. Y. Hakura, Radio Research Laboratories for his useful suggestions and discussions.

#### References

- (1) Obayashi, T. and Y. Hakura, (1960) : Report Ionos. Space Res. Japan, 14, 1.  
Hakura, Y., (1961) : Doctor thesis, Quarterly Reveiw of Radio Res. Lab., Special issue.
- (2) Obayashi, T., (1958) : Res. Ionos. Res. Japan, 12, 301
- (3) Nagata, T. and S. Kokubun, (1962) : Nature Vol. 195, No. 4841.
- (4) Chapman, S., (1953) : Terr. Mag. Atmos. Elect., 40, 349  
Hasegawa, M., (1940) : Trans. Washington Meeting, A.T.M.E., I.U.G.G., 311  
Vestine, E.H., (1940) : Trans. Washington Meeting, A.T.M.E., I.U.G.G., 360  
Harang, L., (1946) : Terr. Mag. Atmos. Elect., 51, 353  
Nagata, T., (1950) : Journ. Geophy. Res., 55, 127
- (5) Sano, Y., M. Nagai, and K. Yanagihara, (1962) : Memoirs Kakioka Mag. Obs. Vol. 2, No. 10

## 1958年2月11日の磁気嵐について

永井正男

## 概 要

1958年2月11日01時25分 UT におこった急始大地磁気嵐について、28観測所の毎時値を使って、急始の24時間前から、48時間後まで Dst 場及び DS 場を解析した。そして DS 場の等価電流ベクトルとブラック・アウトの汎世界的パターンとを比較検討した結果、次に示す3つの特性が明らかになった。

(1) SCの直後(+1時)に極めて顕著な DS 場が、極光帯及び極冠帯のほとんど全領域においてみられた。これは通常の地磁気嵐が Dst 場の発達につれて、DS 場も次第に発達するのに比べ、ほとんど例外的といってよいほど特徴的である。

(2) ブラック・アウトの始まった急始前13時間において、それまで全く静穏であった地磁気が活動を開始し、ブラック・アウトの発達につれて-6時間では、College, Tiksy, Dixon で-500 $\gamma$ の地磁気擾乱を観測した。Pre-SC 擾乱の電流系は午前側では時計廻り、午後側では反時計廻りで、初相における電流系は Pre-SC 擾乱の電流系が強調されたものである。

(3) Dst 場の発達にともなって極光帯の南下が顕著にみられる。Dst 場の極大時(+9時)を境にして発達過程においては午前側のヨーロッパゾーンにおいて、回復過程においては23時~20時のアラスカ~カムチャッカゾーンにスパイラルに南下し、地磁気緯度 34.1° の女満別において LT 19時~22時に極光が観測された。